

## A Maintenance-Free Battery Charge Control Approach for Nickel-Hydrogen Batteries

Andrew W. Lewin  
Principal Systems Engineer  
Orbital Sciences Corporation  
Dulles, VA 20166  
(703) 406-5000  
lewin.andy@orbital.com

**Abstract.** The most common battery charging approaches for nickel-hydrogen batteries suffer from two key limitations. They either consistently under- or overcharge the battery or they require accurate knowledge of the battery capacity. For the ORBCOMM constellation of 36 small communications satellites, regular overcharging is unacceptable because it decreases battery life. Worse, the lost life occurs when the satellite constellation is facing its greatest usage demand. On the other hand, obtaining an accurate knowledge of the battery capacity requires an upfront effort to develop the necessary engineering tools and characterize battery performance. In addition, the satellite operator must bear the recurring expense of continuously estimating the capacity over the 5-year design life of each spacecraft.

To avoid these limitations, the ORBCOMM system employs a patented battery charging approach that estimates the battery charging efficiency by computing the amount of charge received by the battery as a function of the input charge. The full point of the battery is easily determined since the charge efficiency drops as the battery charge approaches its capacity. The battery charge is estimated by computing the moles of  $H_2$  gas in the cell; the input charge is simply the integral of the charge current. So, the charge efficiency is proportional to the rate of change of the moles of  $H_2$  gas with respect to the input charge, or  $dM/dC$ . This maintenance-free approach enables the charging routine to perfectly fill the batteries—without overcharging— independent of the battery capacity.

Any algorithm based upon a derivative estimate poses a noise rejection challenge. The  $dM/dC$  approach is no different. The battery charge control system must be adept enough to respond to decreases in  $dM/dC$  yet stable enough to avoid the inherent signal to noise problem at low charge rates. The effectiveness and pitfalls of the  $dM/dC$  battery charge algorithm are highlighted using data from the 26 ORBCOMM constellation spacecraft launched between December 1997 and September 1998.

### Introduction

When designing satellite constellations, the sheer number of spacecraft to be managed dictates the need to include features to improve operability. On the ORBCOMM satellite power system, this has motivated the desire for a maintenance-free battery charging scheme. This imposes several key requirements. First, the charge control approach must be capable of autonomous initialization. Second, the system has to adapt to long-term changes in the battery performance over the five-year satellite design life.

### Charge Control Concept

To satisfy these requirements, the battery charge control approach must depend upon measurable properties that do not change over the lifetime of the spacecraft. The ORBCOMM battery charge control approach relies upon the relationship between the battery state of charge and the charge efficiency. When a battery is

partially depleted, the majority of an input charge is stored in the battery. In  $NiH_2$  batteries, this is observed as an increase in the amount of hydrogen gas present in the cell. As the battery reaches its full point, a greater percentage of the input charge is converted to heat, while less is stored in the battery. Thus, the battery fullness can be determined by estimating the amount of charge accepted by the battery as a function of the input charge.

Since the battery state of charge is directly related to

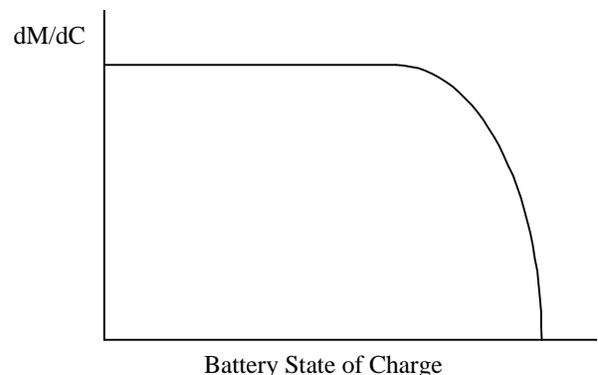


**Figure 1:** Relationship Between  $dM/dC$  and the Battery State of Charge

the moles of hydrogen gas present in the cell, the change in battery charge is proportional to the change in input charge. Thus, the battery current command is driven by the change in moles by the change in input charge. Expressed as a derivative, this value is  $dM/dC$ . Figure 1 shows the relationship between  $dM/dC$  and the battery state of charge.

Figure 1 shows that  $dM/dC$  is constant for nearly all battery states of charge. As the battery approaches its full point, less of the input charge ( $dC$ ) is stored in the battery ( $dM$ ), so  $dM/dC$  decreases. In the limiting case, the entire input charge is converted to heat; none is stored in the battery, so  $dM/dC$  is zero.

### **dM/dC Battery Charge Control Approach**

As shown in Figure 2, the battery charge control system consists of two parts, an estimator and a controller. The estimator is responsible for determining the battery state. In this case, the battery state is given by the value of  $dM/dC$ . The controller is responsible for computing the appropriate charge current based upon the current battery state.

#### **dM/dC Estimator**

Implementation of the  $dM/dC$  charge approach requires an estimate of the change in moles of hydrogen gas and the battery input charge. The moles of hydrogen gas are calculated using pressure and temperature measurements and the ideal gas law:

$$m = \frac{PV}{RT}, \quad dm = \frac{V}{R} d\left(\frac{P}{T}\right)$$

Since  $V$  and  $R$  are constant, they are immaterial to the derivative. Therefore, the algorithm uses scaled moles, denoted by the symbol  $M$ :

$$M = m \frac{R}{V} = \frac{P}{T}, \quad dM = d\left(\frac{P}{T}\right)$$

The input charge is simply the integral of the input current:

$$C = \int I_{\text{bat}} dt, \quad dC = I_{\text{bat}} dt$$

Thus,

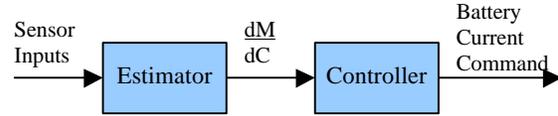


**Figure 2:** Battery Charge Control Algorithm Elements

$$\frac{dM}{dC} = \frac{d\left(\frac{P}{T}\right)}{I_{\text{bat}} dt}$$

The equations above form the mathematical basis of the  $dM/dC$  algorithm. However, putting the concept into practice presents some interesting challenges. In particular, any algorithm relying upon a derivative calculation has difficulty with noise rejection. The  $dM/dC$  approach is no exception. The objective is to quickly recognize changes in  $dM/dC$  while rejecting the high-frequency noise content of  $dM$ , and to a lesser degree,  $I_{\text{bat}}$ .

The heart of the  $dM/dC$  estimator is a derived rate estimator. The derived rate estimator is a two-state filter that feeds back the current  $dM/dC$  estimate for use in the next estimate of  $M$ . The filter is achieved with the following equations:

$$\hat{M} = \hat{M}_{\text{old}} + k_1 \left( M_{\text{meas}} - \hat{M}_{\text{old}} \right) + \frac{\hat{dM}}{dC_{\text{old}}} I_{\text{bat}} dt$$

$$\frac{\hat{dM}}{dC} = \frac{\hat{dM}}{dC_{\text{old}}} + k_2 \left( \frac{M_{\text{meas}} - \hat{M}_{\text{old}}}{I_{\text{bat}} dt} \right)$$

The derived rate filter alone provides a good estimate of  $dM/dC$ . However, a first-order lag function (low pass filter) is applied to the output of the derived rate filter to further reject high-frequency noise. In equation form, the low pass filter is:

$$\frac{\hat{dM}}{dC_f} = (1 - k_3) \frac{\hat{dM}}{dC_{f_{\text{old}}}} + k_3 \frac{\hat{dM}}{dC_f}$$

To examine the behavior of the resulting estimator, the equations are combined and expressed in matrix form:

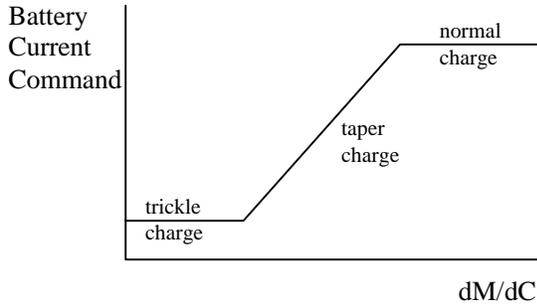


**Figure 3: dM/dC Controller**

$$\begin{bmatrix} \hat{M} \\ \frac{d\hat{M}}{dC} \\ \frac{d\hat{M}}{dC_f} \end{bmatrix} = \begin{bmatrix} 1-k_1 & I_{bat} dt & 0 \\ -\frac{k_2}{I_{bat} dt} & 1 & 0 \\ 0 & k_3 & 1-k_3 \end{bmatrix} \begin{bmatrix} \hat{M}_{old} \\ \frac{d\hat{M}}{dC}_{old} \\ \frac{d\hat{M}}{dC_{f,old}} \end{bmatrix} + \begin{bmatrix} k_1 \\ \frac{k_2}{I_{bat} dt} \\ 0 \end{bmatrix} M_{meas}$$

The eigenvalues of the 3x3 matrix yield the poles of the estimator. Of course, there is a single zero at the origin (representing the derivative). In terms of the gains  $k_1$ ,  $k_2$ , and  $k_3$ , the poles are located at:

$$1 - \frac{k_1}{2} \pm \sqrt{\left(\frac{k_1}{2} - 1\right)^2 - 1 + k_1 - k_2}$$

$$1 - k_3$$

The placement of the real component of the poles determines the frequency response and time lag characteristics of the dM/dC charge algorithm. As the poles move closer to one, the filter suppresses lower and lower frequencies. This produces an increasingly smooth and consistent estimate of dM/dC, but it comes at the cost of increased filter response time. This response time is important for batteries because a delayed response can lead to battery overcharging, which stresses the cells and reduces battery life.

### dM/dC Controller

As shown in Figure 3, the dM/dC controller is quite simple. The commanded battery charge current is linearly related to dM/dC, with defined upper and lower limits. For most of the charge cycle, the battery is charged at its normal rate. A rate of C/2 is typical, where C is the capacity of the battery in ampere-hours. As the battery approaches its full point, the charge efficiency—and therefore dM/dC—drops. The battery current command drops as well. This reduction in the battery charge rate is called the taper charge. Once the battery is full, the controller maintains a small trickle

charge to ensure that the battery remains fully charged. Trickle charge rates vary from about C/30 to C/100.

### dM/dC Initialization

The dM/dC algorithm must be capable of autonomously determining its state at initial power-up or following a processor reset. Since dM/dC is not estimated during discharge, dM/dC must also be initialized after each eclipse cycle. The battery can be at any state of charge when the algorithm begins. Therefore, the initialization process must balance two competing priorities. The approach must quickly begin recharging a depleted battery while at the same time it must not overcharge a full battery.

The dM/dC estimator consists of three states, M, dM/dC, and dM/dC<sub>f</sub>. On the first cycle, M is set to the current value of P/T, and dM/dC and dM/dC<sub>f</sub> are set to the transition point from trickle charge to taper charge. This point is selected so that if the battery is empty, the dM/dC estimate will rise, and the battery charge current will increase as well, yet if the battery is full, the dM/dC estimate will decline and the battery will not be overcharged. For the next few measurements, M is estimated with a simple low-pass filter with a short time constant in order to establish a good initial estimate. Both dM/dC and dM/dC<sub>f</sub> are held constant during this period. Once this first stage initialization is complete, the estimator begins operating normally.

Controller behavior is also modified during the initialization period. In trickle charge, both dM and dC are small. This significantly reduces the signal to noise ratio on the dM/dC calculation. Therefore, the controller sets a minimum charge rate during the initialization period. This charge rate is chosen to be the highest current that can be safely applied to a full battery. During the second initialization phase, the estimator acts as normal, but the controller applies the

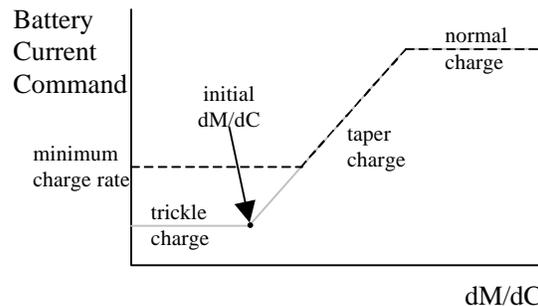


**Figure 4: dM/dC Controller During Initialization** higher minimum charge rate. The initialization con-

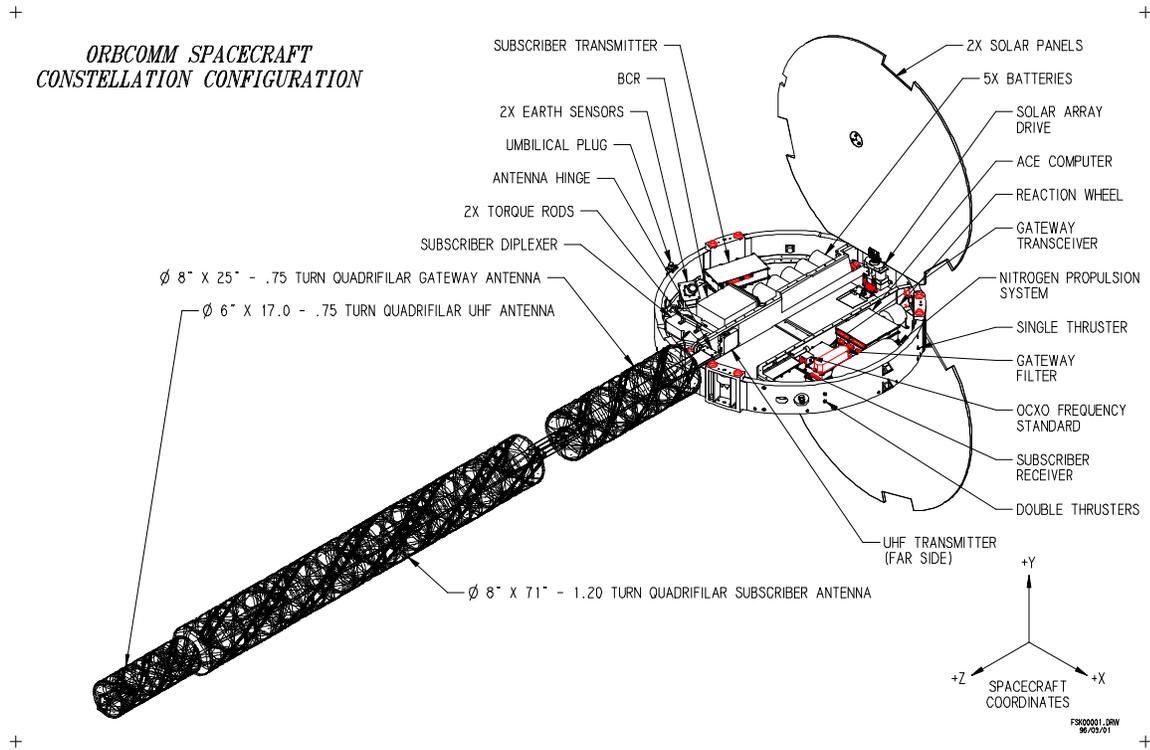


**Figure 2: ORBCOMM Spacecraft**

troller is shown by the dotted line on Figure 4. The gray line is the standard dM/dC controller. The length of the overall initialization period must be selected to be on the order of the time constant of the estimator to ensure an accurate initial estimate.

**Battery Charge Control on the ORBCOMM Constellation Spacecraft**

**ORBCOMM Hardware Configuration**

A diagram of the ORBCOMM spacecraft is shown in Figure 5. The ORBCOMM battery pack consists of five 10 A-hr nickel-hydrogen (NiH<sub>2</sub>) common pressure vessels (CPV) with two cells per CPV. The battery pack has a nominal voltage of 14V for a nameplate capacity of 140 W-hr.

The spacecraft provides a battery voltage and a highly accurate battery current measurement. A strain gage and temperature sensor are mounted on the second and fourth CPVs. The CPVs in each pack are carefully selected to ensure that the cells are as closely matched as possible.

Battery thermal control is provided by a radiator and actively controlled heaters. The thermal design is slightly cold-biased to maximize battery capacity and

therefore battery life. The CPVs are mounted to a radiator plate that nominally points normal to the sun line. The battery radiator also extends up the wall of the antenna trough to provide extra area. To avoid inducing large temperature gradients in the battery cells, the battery heater is mounted on the radiator.

**Battery Charge Control Software**

The ORBCOMM battery charge control software modes are depicted in Figure 6. These modes also drive spacecraft power management. During nominal operation, the battery charge control is in Normal mode, which uses the dM/dC algorithm.

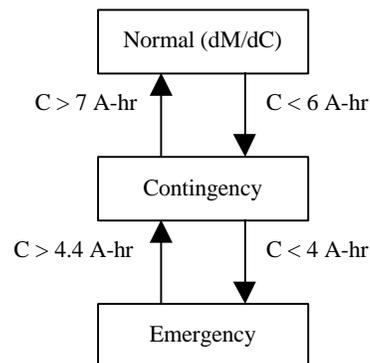


**Figure 6: ORBCOMM Power System Modes**

The dM/dC algorithm can only tell when the battery is getting full; it cannot determine the depth of discharge of the battery. Therefore, the battery charge mode transitions are performed based upon a separate estimate of the battery charge. Manufacturer data is used to convert the battery pressure and temperature into a coarse estimate of the battery charge. This enables the satellite software to identify anomalous situations. If the battery charge drops below 6 A-hr the spacecraft takes steps to decrease power consumption and increase power generation. The software also increases the battery charge command to 9A. By comparison, the battery charge command is limited to 5A (C/2) during dM/dC operation.

If the battery charge continues to fall, the battery charge mode drops to Emergency. The power system software removes power from all non-essential loads. The battery charge command remains at 9A. In Contingency and Emergency modes the dM/dC software continues running in the background. The algorithm estimates dM/dC so that no initialization is required when the battery control software mode returns to Normal.

### **Developing the dM/dC Charge Algorithm**

The basic premise of the dM/dC battery charge algorithm is quite straightforward; however, the first step was to determine whether the approach would work on a real battery. Early control system development typically starts with a software model of the system being controlled. In this case, however, software simulation was largely omitted. This was done for two reasons: (1) the target processor, battery charge electronics, batteries, and EGSE were already available and (2) it would be too difficult and time-consuming to develop a battery model with sufficiently high fidelity to establish the feasibility of the dM/dC battery charge control approach.

Most algorithm development was performed using the ORBCOMM engineering development unit (EDU) spacecraft. The EDU is comprised of non-flight versions of nearly all flight hardware, including the NiH<sub>2</sub> batteries. The high fidelity of this model was very important to the development effort. Once the algorithm was perfected on the EDU spacecraft, it could be transferred to the flight units without modification.

By and large, the algorithm development went quite smoothly. The dM/dC charge control method was al-

most immediately shown to be feasible. Figure 7 shows a typical charge profile taken from one of the early EDU tests. The algorithm correctly recognizes that the battery is not full and begins charging at the maximum rate. As the battery approaches its full point, the value of dM/dC begins to decline and the algorithm reduces the charge rate. The software then maintains a constant trickle charge to ensure that the battery remains full.

Once the basic operation of the dM/dC charge algorithm was established, it was run through a wide variety of test cases. One series of tests evaluated charging for very low depth of discharge (DOD) cycles. These tests determined whether the initialization routine selected the correct initial charge rate. These tests went quite smoothly. Based upon the test results, the initialization routine was modified slightly to provide optimum performance.

Another extensive series of tests evaluated battery performance in the presence of temperature transients. For these tests, a battery pack was placed in a small thermal chamber with the power system electronics on a test bench nearby. The first set of tests was performed at constant temperature ranging from -7°C to ambient (22°C). The battery underwent several charge cycles of varying DOD at each temperature threshold. These tests showed that—as expected—dM/dC performance did not vary over temperature.

After verifying performance at constant temperature, the tests were repeated during temperature transients. First, the battery was placed at cold (-5°C to -7°C) for at least an hour to achieve thermal stability. Then the chamber temperature was raised at rates up to 20°C/hour. The chamber temperature was then held at a warm plateau (about 20°C) for at least an hour to reach steady-state. Finally, the chamber temperature was reduced at the same rate at which it was raised. The battery underwent at least one charge/discharge cycle during each transient.

Of course, the dM/dC development and testing effort turned up several issues.

#### *Battery Pressure Measurement*

As a derivative-based algorithm, dM/dC is very sensitive to accuracy of the measurement of the battery temperature and pressure. The dM/dC unit-level testing turned up two issues with the battery pressure measurement.

First, the battery pressure measurement exhibited a slight jump when the battery heater was enabled. Under normal circumstances, this behavior would probably have gone unnoticed. However, the jump in P, without a corresponding increase in T, causes a step

change in M. Since the change happens nearly instantaneously, the large  $dM$  is divided by a relatively small change in  $dC$ , and the  $dM/dC$  estimate is artificially high. This results in a higher than desired battery charge current.

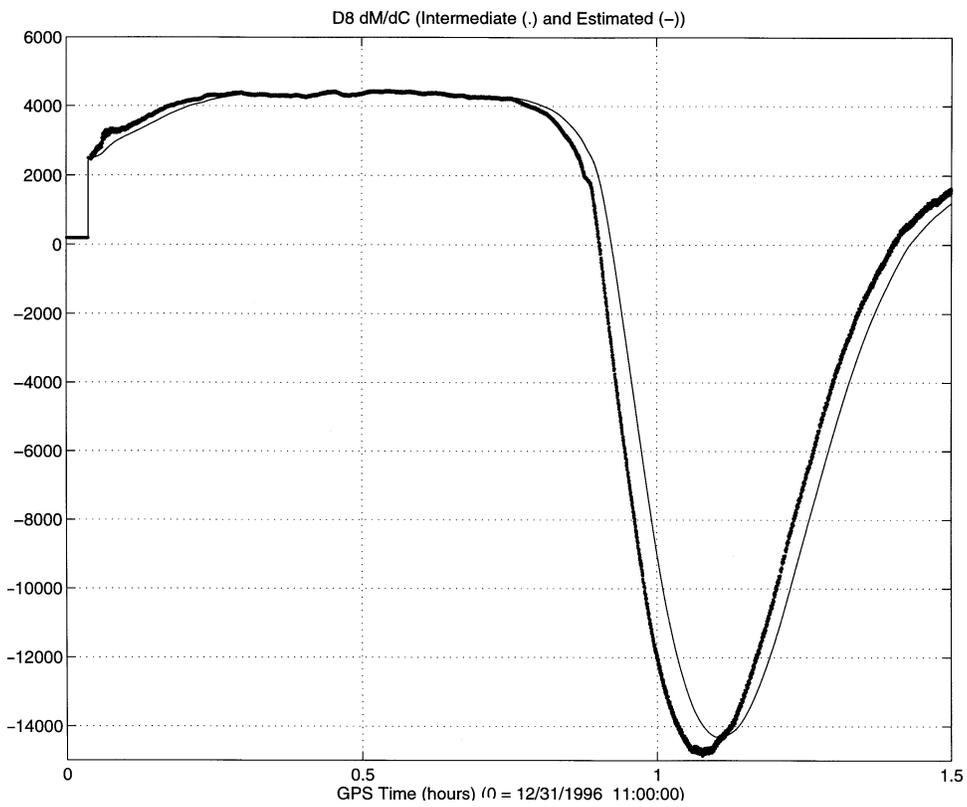
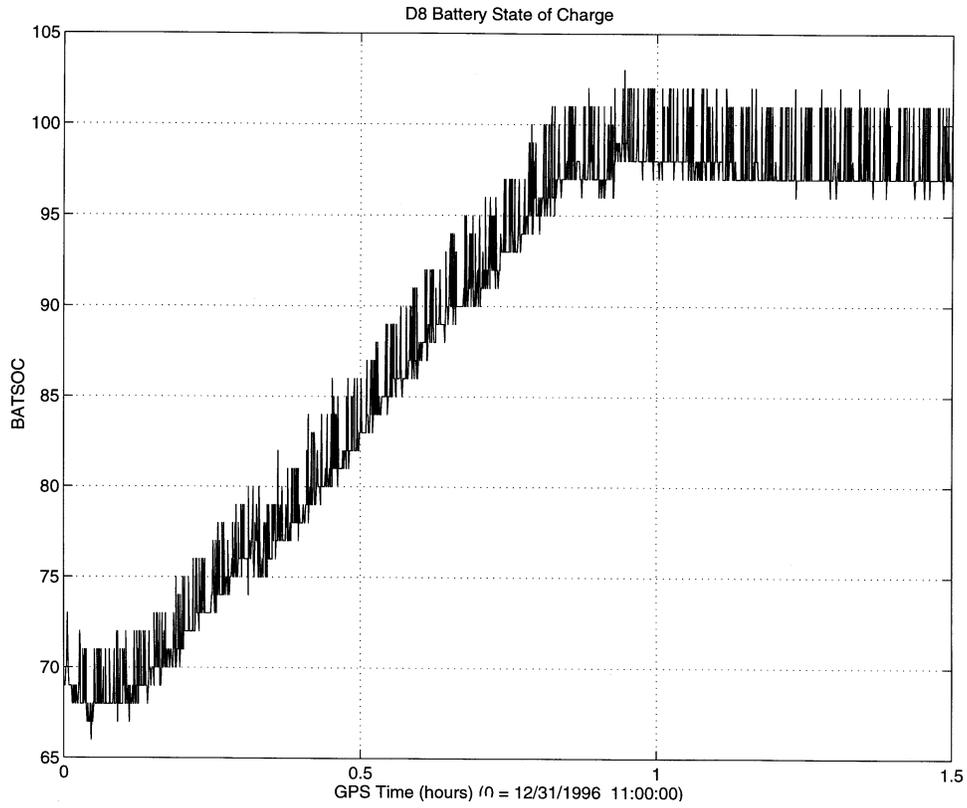


Figure 7: dM/dC Early Algorithm Development Test Data

If such an event occurs when the battery is nearly full, it can cause a damaging overcharge. The algorithm eventually damps the transient induced by the step change. The reverse process occurs when the battery heater is turned off.

This problem was easily overcome. Further testing demonstrated this behavior in all power electronics. Therefore, the power system software was modified to automatically compensate for the step change in the battery pressure.

The second difficulty encountered in the test program was that the battery pressure measurement was not properly calibrated over temperature. Since the battery pressure did change over temperature, this problem is nearly impossible to spot in real time. The problem was discovered during spacecraft-level thermal testing when the dM/dC estimate was outside its normal operating point during thermal transitions.

The source of the problem became apparent from a plot of battery pressure versus battery temperature. The curve did not follow the ideal gas law. Testing was then performed on several flight and ground test battery packs to establish the consistency of the battery pressure sensor measurement over temperature. These tests showed that a single calibration could be used for all battery packs. This was an important result because calibration of each battery pack would have been time-consuming and expensive.

#### Signal to Noise

Once the battery is full, the battery charge rate is set to a small trickle charge. On the ORBCOMM spacecraft, the trickle charge is 0.3A (C/33). The difficulty with trickle charge is that both dM and dC are small. Furthermore, the quantization of the battery current (dC) is 0.07A, or almost 25% of the desired current. Therefore, the dM/dC estimate is extremely noisy.

Over long times, the noise in the dM/dC measurements periodically causes the algorithm to exit trickle charge and begin charging at a higher rate. This leads to undesirable battery overcharging. The ORBCOMM satellites can go through periods of several days of no eclipse orbits where the battery remains in trickle charge, so long-term trickle charge performance is important.

This problem had a straightforward solution. The dM/dC gains were made a function of the dM/dC estimate itself. When dM/dC—and therefore the battery

charge current—is high, the gains are set higher. When dM/dC is low, the gains are reduced. This has advantages in both scenarios. The high gains at high charge rates allow the algorithm to more rapidly respond to the battery as it gets full. During trickle charge, the low gains prevent the charge algorithm from accidentally transitioning to higher charge rates.

#### Battery Temperature

One of the greatest challenges of the dM/dC algorithm turned out to be the battery temperature measurement. However, to appreciate the limitations of the temperature sensing, one must first understand the battery thermal design. The battery CPVs are held by a metal sleeve wrapped around the center of the CPV. This sleeve is mounted to a baseplate that is cured into the spacecraft bus shelf. Heat is conducted through this sleeve into the baseplate, which serves as a radiator to deep space. This radiator extends up the side of the antenna trough to provide additional heat rejection. Finally, the batteries are wrapped with several layers of a special material designed to minimize the magnetic field created by the batteries during charge and discharge.

The battery thermal design is cold-biased. By keeping the battery temperature low (-5 to 0C), battery capacity is maximized, which reduces the depth of discharge and maximizes battery life. Heaters are employed in order to keep the batteries from freezing. The heaters are placed on the baseplate. This minimizes the thermal gradient across the CPVs.

The battery pressure is measured by a strain gage mounted to the outside of the CPV. This sensor responds almost instantaneously to changes in the battery pressure. The battery temperature sensor is also located on the outside of the CPV. This poses a problem, since changes in the cell temperature must propagate through the walls of the CPV before reaching the sensor.

This explains the somewhat surprising behavior of the battery at the end of the charge cycle. When the battery gets close to its full point, less and less of the input charge is stored in the battery. The remainder is rejected as heat. Therefore, the battery pressure increases more slowly, and the battery temperature begins to rise. Figure 8 shows that the temperature and pressure exhibit this behavior; however, the battery temperature increase is measured later than the deceleration of the battery pressure growth, even though they actually occurred at the same time.

This explains why the estimate of moles (M) appears to

However, this solution is not feasible because the temperature sensor has the opposite problem in response to

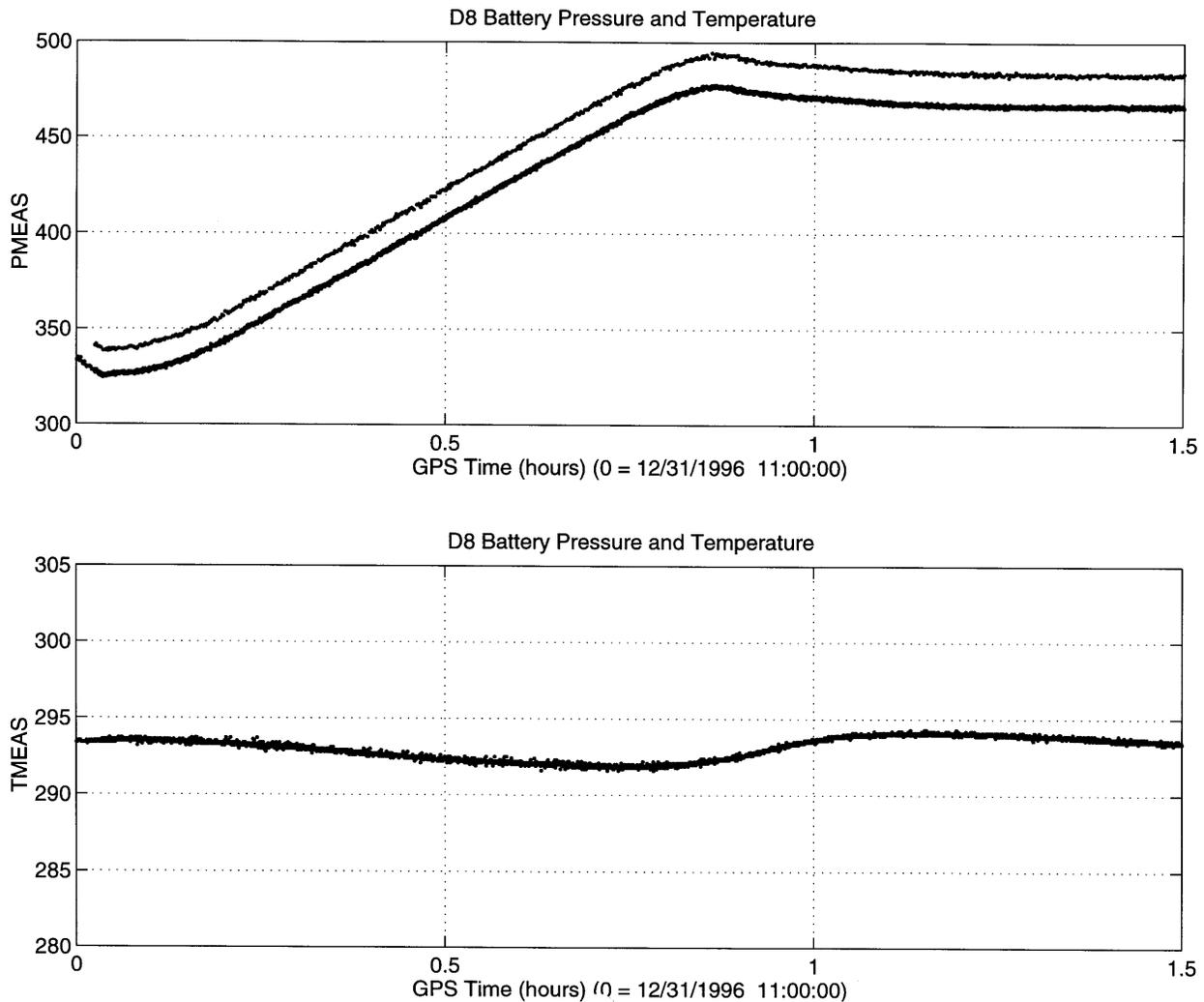


**Figure 8:** Battery Temperature and Pressure Profiles During Charging

decrease even though the battery charge current is positive. The lagged temperature increase occurs when the battery pressure has leveled off, so P/T decreases, creating the theoretically impossible negative values of  $dM/dC$  seen in the plot.

This behavior is undesirable because the lag in the temperature measurement causes the algorithm to delay its reaction to a full battery. As a result, the battery is subjected to a slight overcharge. An obvious solution to this problem would be to add lead to the temperature measurement. This would bring the pressure and temperature measurements in sync and optimize the battery charge profile.

external stimuli. When the battery heaters are enabled or spacecraft pointing errors cause unexpected heat input to the radiators, the temperature sensor observes the change in conditions before they have affected the cell temperature. In this case, the battery temperature sensor measures a temperature increase, while the actual battery pressure and temperature are still unaffected. This increase in T creates a decline in  $dM/dC$ , causing the battery to be charged at a less than ideal rate. This situation calls for the battery temperature sensor to be lagged. So, since some situations prefer temperature lead, and others demand temperature lag, the only option is to use the temperature measurement without modification.

The only way to solve this problem is to closely couple the temperature sensor to the cell temperature. Ideally, this requires a temperature sensor to be placed inside the CPV. This approach is difficult to manufacture and was not considered for the ORBCOMM program.

Although the problem cannot be totally eliminated, several workarounds are available. The slight overcharge caused by the lag in the cell temperature measurement can be mitigated by increasing the value of dM/dC used to transition from normal to taper charging. Increasing the trickle charge transition point helps as well.

The problems caused by external stimuli can also be addressed. Externally-caused temperature increases cause dM/dC to dip below the correct value. During trickle charging this has no effect. In normal charging the battery charge current is decreased. This is only a problem if the spacecraft has a small power or charging margin. In this case, the problem is overcome by increasing the maximum battery charge rate to compensate for the lost charge caused by the event.

External temperature decreases cause the opposite effect. If this occurs during normal charging, dM/dC increases but the battery charge remains at the normal charge rate. If it occurs during trickle charging, the battery will receive an unwanted charge. This is overcome through the implementation of a trickle charge locking mechanism. If the battery charge command remains in trickle charge for a minimum amount of time, the battery charge rate is locked at trickle charge regardless of the value of dM/dC. This causes the system to ignore the externally-caused transient event.

### **On-Orbit Performance**

Through rigorous ground testing, the dM/dC charge algorithm was demonstrated to be an effective method for battery charge control. However, there was some uncertainty about how the system would perform in the space environment. The moment of truth came with the launch of the first eight ORBCOMM spacecraft on 23 December 1997. In the end, dM/dC performance very closely matched the ground test data.

Figures 9 to 12 show the battery charging performance for satellites in each of the four planes of ORBCOMM constellation spacecraft. The upper plot shows the battery recharge cycle, while the bottom plot shows the battery charge current command and the current actually delivered. The satellites were selected to show a variety of battery capacities and depths of discharge.

The figures show that the dM/dC battery charge control algorithm accurately initializes its charge state and correctly reduces the charge current as the battery approaches its full point. The dips in the battery charge current are indicative of the noise in the dM/dC estimate. They could be eliminated by selecting a higher transition point from normal to taper charging in the dM/dC controller; however, this is not necessary for the ORBCOMM application. In addition, the lower setpoints decrease the likelihood of battery overcharging.

The only significant difference observed from ground testing was that the battery charge efficiency in space was slightly better than that on the ground. In other words, dM/dC was slightly higher than anticipated. The battery charge control parameters were easily modified to raise the trickle and taper charge transition points slightly.

The greatest result is the flexibility of the dM/dC charge algorithm. The data presented shows battery recharge events ranging from about 3.5 A-hr to less than one amp-hour. Over the course of all flight operations, the charge control algorithm has operated correctly for even higher depths of discharge. More importantly, the dM/dC approach works—without modification—on batteries with capacities that vary by more than 10%. Furthermore, the charge algorithm has lived up to its claim of being maintenance-free. No battery characterization has been required as the batteries have aged.

### **Conclusion**

The performance of the dM/dC charge algorithm has been proven in orbit. The algorithm is currently flying on 28 satellites (26 ORBCOMM, BATSAT, MUBLCOM) in six orbital planes with four different inclinations. As of August 1999, the dM/dC approach has executed more than 175,000 charge cycles. In this time, the algorithm has been subjected to an endless variety of operating conditions. It has successfully responded to all of these cases, demonstrating the robustness of the dM/dC algorithm.

Overall, the dM/dC battery charge control algorithm proved to be an ideal solution for the ORBCOMM satellites. It successfully optimizes battery charging while eliminating maintenance of the battery charge control software. This makes the dM/dC approach perfect for applications requiring peak performance or low-cost operations.

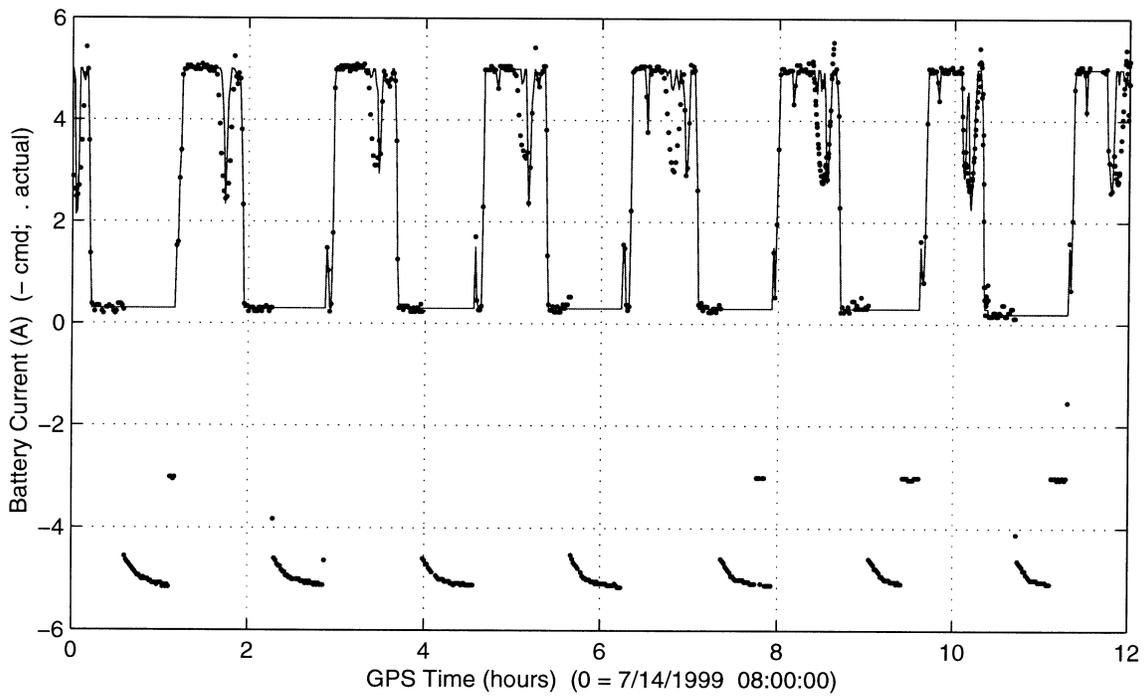
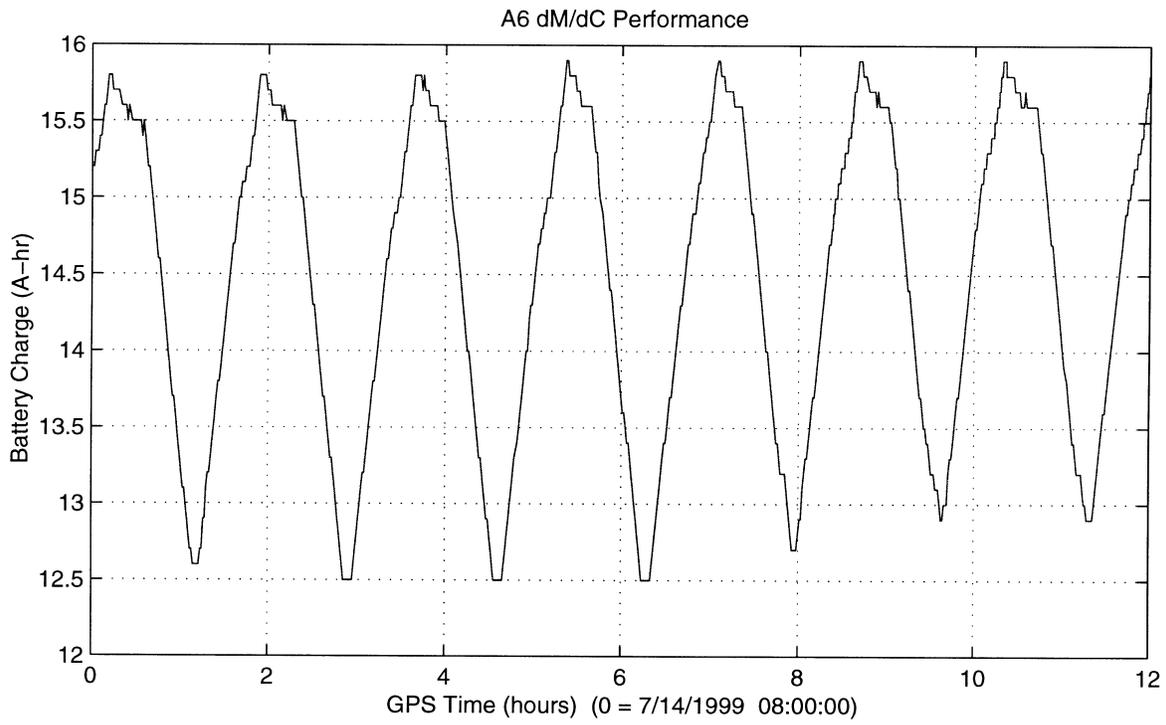
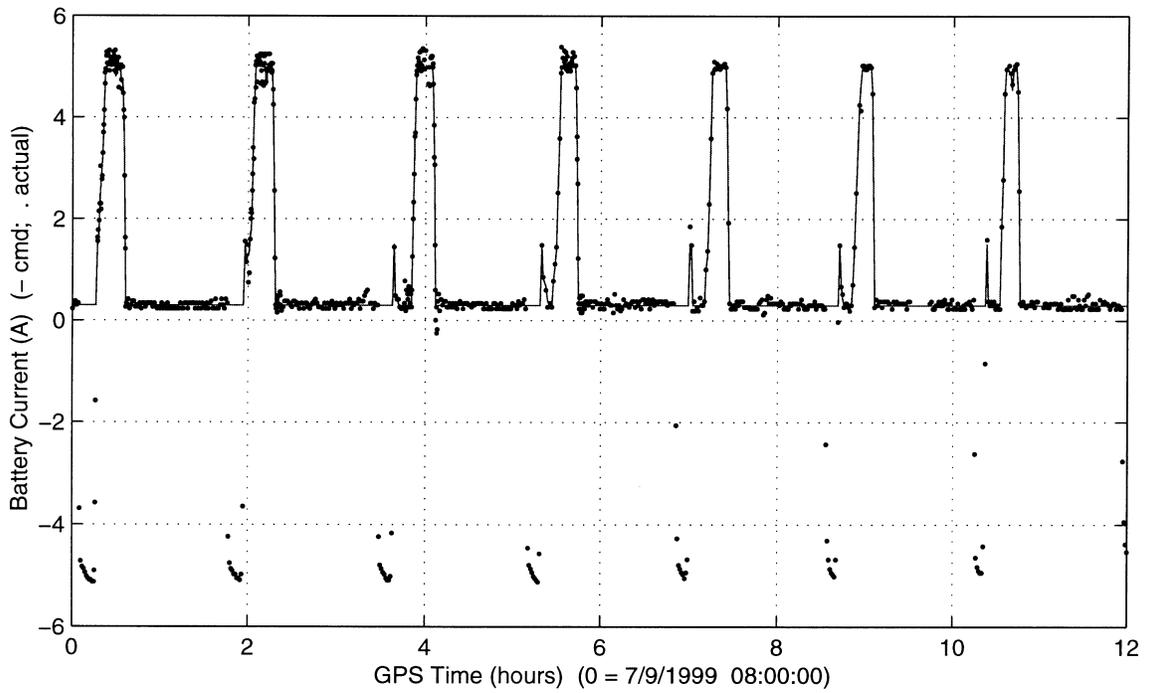
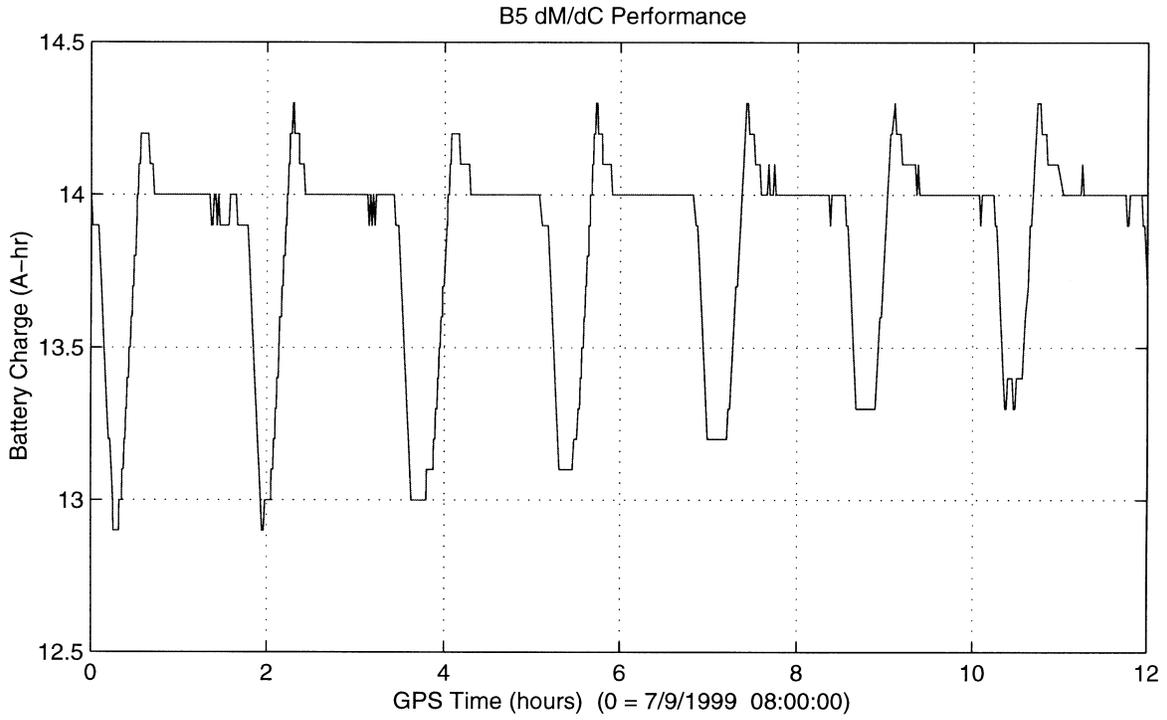
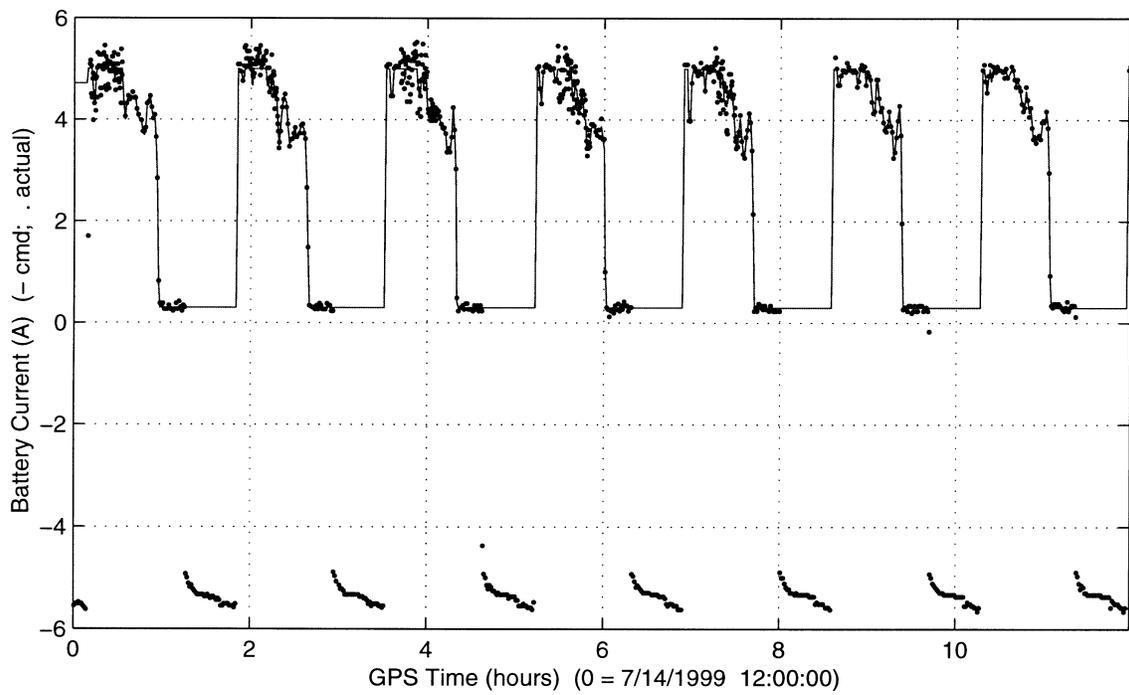
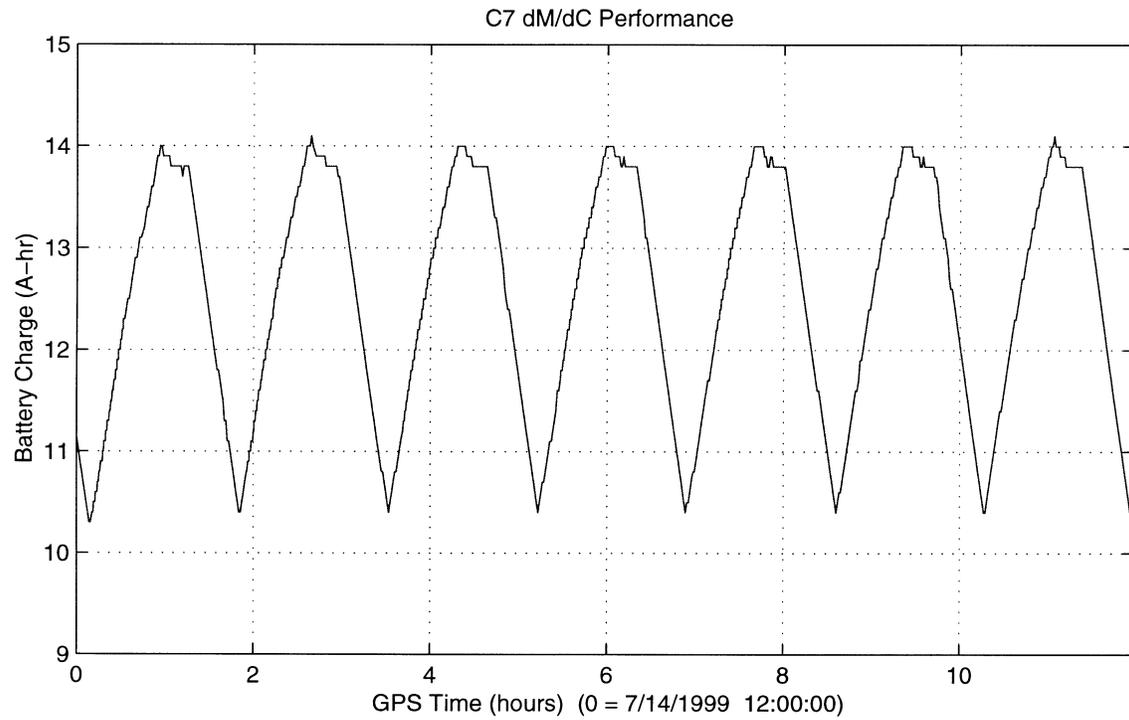


Figure 9: On-Orbit dM/dC Performance for ORBCOMM Satellite A6



**Figure 10:** On-Orbit dM/dC Performance of ORBCOMM Satellite B5



**Figure 11:** On-Orbit dM/dC Performance of ORBCOMM Satellite C7

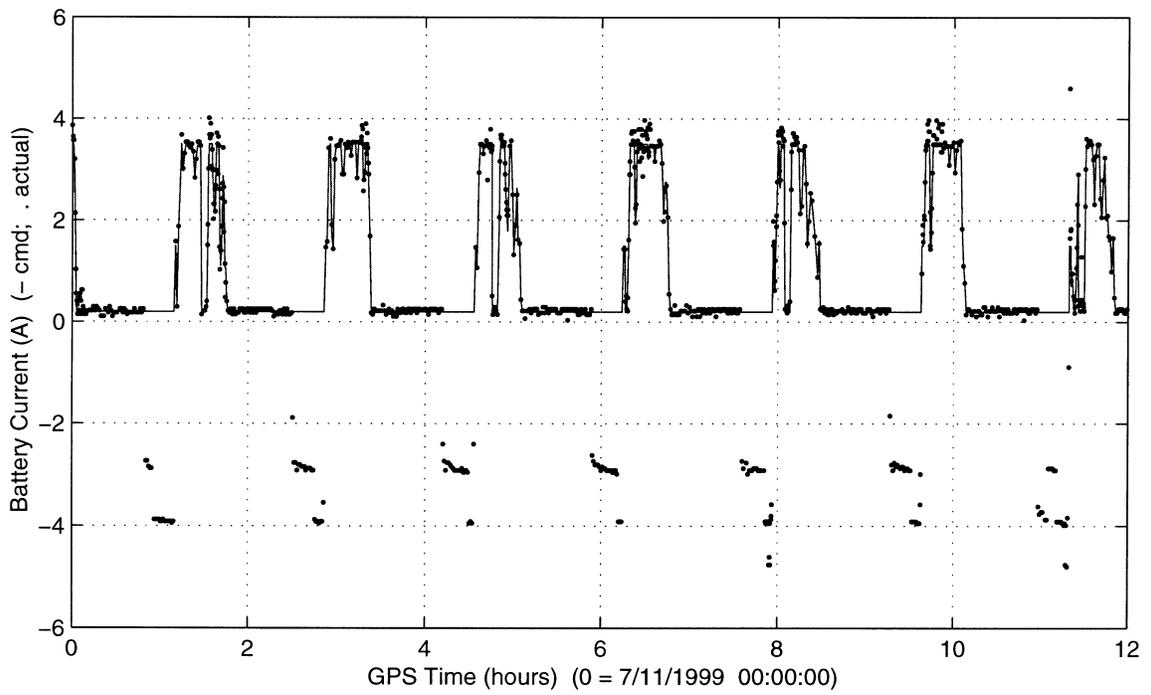
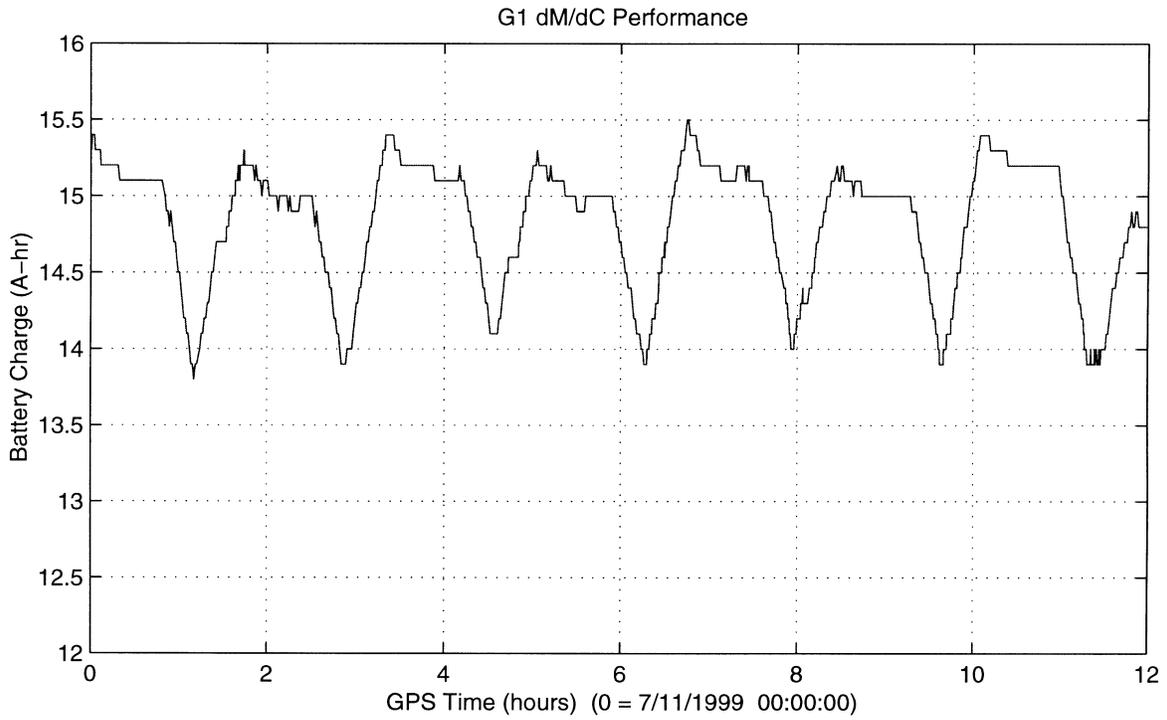


**Figure 12:** On-Orbit dM/dC Performance of ORBCOMM Satellite G1